

## A Parallel Mechanism for Tracking the Sun

R.B. Ashith Shyam, Ashitava Ghosal

Department of Mechanical Engineering, Indian Institute of Science, Bangalore, 560012, India  
email: ashith@mecheng.iisc.ernet.in, asitava@mecheng.iisc.ernet.in

**Abstract:** In concentrated solar power (CSP) power generating stations, solar energy from a large number of mirror systems, also called heliostats, is concentrated at a receiver and the thermal energy in the solar radiation is converted to electricity. Typically, the sun's motion is tracked by using the well-known Azimuth-Elevation method or by the Target-Aligned or Spinning-Elevation method. In both these approaches of tracking, the mirror needs to be moved about two axis independently, using two actuators, in a way such that the reflected sun's radiation is concentrated on a far away receiver in the solar field. In both the methods, the two actuators are in series and the mirror is effectively mounted at a single point. In this paper, we propose the use of a three degree-of-freedom parallel manipulator, namely the 3-RPS parallel manipulator, to track the sun. The proposed 3-RPS parallel manipulator supports the load on the mirror at three points, and hence much larger mirror can be moved with the required tracking accuracy and without increasing the weight of the support structure. We present the kinematics equations used to determine motion of the actuated prismatic joints in the 3-RPS parallel manipulator such that the sun's rays are reflected on to a stationary receiver. We present kinematic and finite element based simulation results which demonstrates the advantages of the proposed parallel manipulator.

**Keywords:** 3-RPS, Parallel manipulator, Heliostat, Solar tracking

### 1 Introduction

Research and development of clean energy systems has been gaining in acceptance and use in the recent past. Solar energy being the most abundant, renewable, non-pollutant and available throughout the year has the highest potential from which clean energy can be harvested. The popular methods to harvest solar energy is the use of photo-voltaic cells, parabolic troughs and dishes, central receiver tower system etc. In this paper, the focus is on concentrated solar power (CSP) approach where the sun's energy is concentrated at a central receiver tower and then converted to electricity. One of the advantages of CSP over other solar energy harvesting approaches is higher efficiency and lower cost [1].

There are two well-known existing methods for concentrating solar energy application. These are called the Azimuth-Elevation and Target-Aligned method [2]. Out of these two, the Azimuth-Elevation method is the most widely implemented one. In both the above methods, there are two actuators which track and orient the mirror system, also called the heliostats, in such a way that the incident ray from the sun is reflected onto a fixed central receiver. The mirrors are supported by using a support frame and a pedestal which is fixed to the ground. Since the pedestal

is typically placed at the geometrical centre of the arrangement of mirrors, the deflection of the support frame and the mirrors due to self-weight and wind load can go beyond the allowable slope error limit of 2-3 mrad [1] at the edges or corner of the mirror structure. In order to tackle this problem, either the support frame has to be made more rigid or smaller sized mirrors have to be used. A larger number of smaller mirrors imply the use of more actuators and sometimes loss of harvested energy due to blocking of one mirror by another.

Both the Azimuth-Elevation and Target-Aligned arrangement are kinematically in a serial configuration and as in any serial configuration, the tracking error is the sum of the errors of the two actuators. To reduce tracking error to less than the required 2 mrad [1], accurate and expensive gear boxes need to be used to achieve the large gear reduction required to track the motion of sun (approximately  $\pi$  radians in 12 hours). In this work, we propose the use of a three-degree-of-freedom parallel manipulator, namely the well-known 3-RPS parallel manipulator. As in any general parallel manipulators, the payload, in this case, the mirror and support structure, can be much larger and the tracking accuracy will be governed by the largest error in an actuator. In spite of the use of extra actuator, as compared to the Azimuth-Elevation and Target-Aligned method, it is expected that the overall cost of the heliostat will be lower with the 3-RPS parallel manipulator.

This paper is organized as follows: in section 2, we present a brief description of the three-degree-of-freedom parallel 3-RPS manipulator, the optics and kinematic equations relating the orientation of the mirror to the motion of the sun in the sky and the motion of the actuated joints required to focus the reflected sun radiation on to a fixed receiver. In section 3, we present the finite element based modeling of the mirror and structure to study the effects of the wind loading and self-weight. In section 4, we present the kinematic and finite element analysis results and demonstrate the advantages of using a parallel manipulator for a heliostat. Finally, in section 5, the conclusions of the work and future directions are presented.

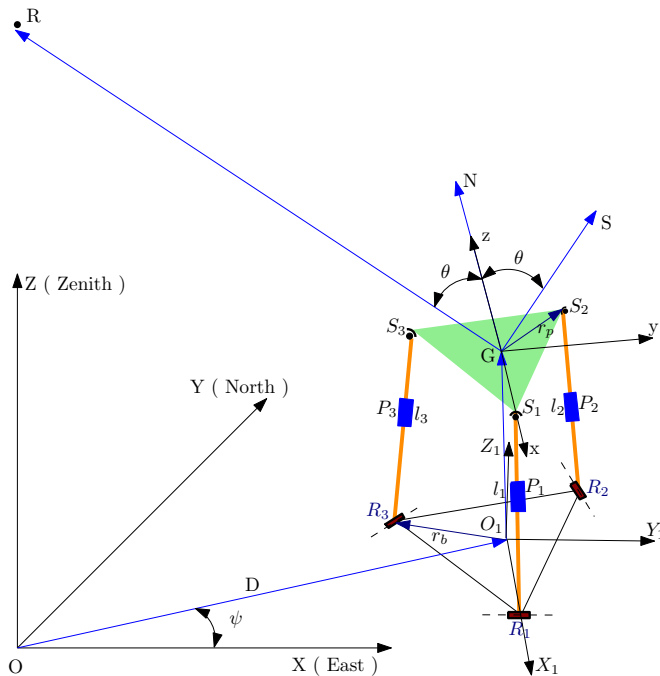
### 2 Geometry and kinematics of a 3-RPS manipulator

Figure 1 shows the well-known three-degree-of-freedom parallel manipulator. It consists of a top moving platform which is connected to a fixed base by means of three actuated prismatic (P) joints. At each of the connection point,  $S_i$ ,  $i = 1, 2, 3$ , to the top moving platform, there is a spherical (S) joint and at each of the connection point at the fixed based there is a rotary (R) joint. The axis of the rotary joints are in the plane of the fixed platform. The mirror assembly is fixed to the top moving platform using a support structure which is designed to provide adequate stiffness such that deflections due to wind loads and self-

weight are within acceptable limits as mentioned earlier. Even though the mirror assembly can have arbitrary shapes, for the purpose of kinematics only the triangle formed by  $S_1$ ,  $S_2$  and  $S_3$  need to be considered.

It can be shown that the 3-RPS manipulator has three degrees of freedom and thus three actuators can be used to move the top platform [3, 4]. It can be further shown that the three principal motions of the top moving platform are rotation about  $X$  and  $Y$  axis and a linear motion along the  $Z$  axis [5]. For tracking the sun, the rotation capability about the  $X$  and  $Y$  axis is used. The linear motion along the  $Z$  axis can be used to bring the mirror assembly down when high wind speeds are present.

Referring to Fig. 1, let  $O$  be the origin of the fixed coordinate system,  $\{X, Y, Z\}$ , attached to the fixed-base (ground) on the surface of the earth. The axes  $OX$ ,  $OY$ , and  $OZ$  point towards local East, local North and the zenith directions, respectively. The foot of the receiver tower,  $R$ , and the origin,  $O$ , of the fixed coordinate system coincides with each other. Without loss of generality, we assume that the triangle formed by the connection points  $S_i$ ,  $i = 1, 2, 3$  form an equilateral triangle whose circum-radius is  $r_p$ . The plane of the moving top platform, containing the mirror assembly, is defined by the normal  $\vec{GN}$  given by the cross product of the vectors  $\vec{S_1S_2}$  and  $\vec{S_1S_3}$ . From the laws of optics, a) the incident ray from the sun and the reflected ray to the receiver both make an equal angle  $\theta$  with the normal  $\vec{GN}$  and b) the incident ray, the normal and the reflected ray lie on a plane.



**Figure 1: Schematic diagram of a 3-RPS heliostat**

Let  $l_1$ ,  $l_2$  and  $l_3$  denote the lengths of the prismatic joints at any instant of time. Without loss of generality, we assume that the revolute (R) joints at the fixed base are placed at the corners of an equilateral triangle whose circum-radius is  $r_b$ . The centroid of this equilateral triangle is  $O_1$  which is at a distance,  $D$ , from  $O$  and at an angle  $\psi$  with respect

to the  $OX$  axis. The co-ordinate system at  $O_1$  with axis  $\{X_1, Y_1, Z_1\}$  is described with respect to the fixed coordinate system by a rotation about  $Z$  axis and a translation along  $\vec{OO_1}$ . The coordinate system at  $G$  is denoted with  $\{x, y, z\}$  and the vector  $\vec{O_1G}$  is denoted by  $[x_c, y_c, z_c]^T$ . The homogeneous transformation matrix  $[T]$  which relates the coordinate system at  $O_1$  and  $G$  can be described by,

$$[T] = \begin{bmatrix} n_1 & o_1 & a_1 & x_c \\ n_2 & o_2 & a_2 & y_c \\ n_3 & o_3 & a_3 & z_c \\ 0 & 0 & 0 & 1 \end{bmatrix}$$

where the column vectors  $(n_1, n_2, n_3)^T$ ,  $(o_1, o_2, o_3)^T$  and  $(a_1, a_2, a_3)^T$  determine the orientation of the moving platform.

## 2.1 Kinematics of a 3-RPS heliostat

Since the 3-RPS has three degrees of freedom and the tracking of the sun requires only two degrees of freedom, one can choose  $z_c$  arbitrarily. The unit vector pointing to the sun is denoted by  $\vec{GS}$  and is obtained by knowing the azimuth and elevation angles<sup>1</sup>. The unit vector from the centre of the moving platform to the receiver is given by  $\vec{GR}$ . The angle bisector which is also the normal to the platform,  $\vec{GN}$  is given by  $\vec{GN} = \frac{\vec{GS} + \vec{GR}}{\|\vec{GS} + \vec{GR}\|}$ . From this observation, the direction cosines  $a_1$ ,  $a_2$  and  $a_3$  are known in terms of the unknowns  $x_c$  and  $y_c$ . We can write the constraint equations as

$$n_1^2 + n_2^2 + n_3^2 = 1 \quad (1)$$

$$o_1^2 + o_2^2 + o_3^2 = 1 \quad (2)$$

$$n_1 a_1 + n_2 a_2 + n_3 a_3 = 0 \quad (3)$$

$$n_1 o_1 + n_2 o_2 + n_3 o_3 = 0 \quad (4)$$

$$o_1 a_1 + o_2 a_2 + o_3 a_3 = 0 \quad (5)$$

The 3-RPS configuration introduces additional three constraints [4] given by

$$y_c + n_2 r_p = 0 \quad (6)$$

$$n_2 = o_1 \quad (7)$$

$$x_c = \frac{r_p}{2} (n_1 - o_2) \quad (8)$$

where  $r_p$  is the distance of the vertices of the moving platform. Thus there are 8 equations in 8 unknowns, i.e.,  $\{x_c, y_c, n_1, n_2, n_3, o_1, o_2, o_3\}$ . From equations (6) and (7),

$$n_2 = o_1 = \frac{-y_c}{r_p}$$

and from equation (8),

$$o_2 = n_1 - \frac{2x_c}{r_p}$$

<sup>1</sup>The azimuth and elevation angle of the sun depends on the time of the day and the latitude and longitude of the place on the surface of the Earth. This is available from websites [6] or from programs available in literature.

Eliminating  $n_2, o_1$  and  $o_2$ , we get

$$n_1^2 + \left(\frac{y_c}{r_p}\right)^2 + n_3^2 = 1 \quad (9)$$

$$\left(\frac{y_c}{r_p}\right)^2 + \left(n_1 - \frac{2x_c}{r_p}\right)^2 + o_3^2 = 1 \quad (10)$$

$$n_1 a_1 - \frac{y_c}{r_p} a_2 + n_3 a_3 = 0 \quad (11)$$

$$-2n_1 \frac{y_c}{r_p} + \frac{2x_c y_c}{r_p^2} + n_3 o_3 = 0 \quad (12)$$

$$-\frac{y_c}{r_p} a_1 + \left(n_1 - \frac{2x_c}{r_p}\right) a_2 + o_3 a_3 = 0 \quad (13)$$

Thus we can arrive at 5 equations in 5 unknowns, i.e., ( $n_1, n_3, o_3, x_c$  and  $y_c$ ) which can be further reduced by substitution and using Bezout's method of elimination. Finally we can get two equations in  $x_c$  and  $y_c$  given in equation (14) and equation (15) below. Equations (14) and (15) are numerically solved for  $x_c$  and  $y_c$  in MATLAB<sup>®</sup> using the in-built routine *fsolve* [7]. The  $x_c$  and  $y_c$  values along with the arbitrarily chosen value for  $z_c$  give the vector  $\overrightarrow{O_1 G}$  at any instant of time. Once  $x_c$  and  $y_c$  are known, then all the other unknowns in the transformation matrix can be obtained.

by  $\overrightarrow{GS_1} = [r_p, 0, 0]^T$ ,  $\overrightarrow{GS_2} = [-\frac{1}{2}r_p, \frac{\sqrt{3}}{2}r_p, 0]^T$  and  $\overrightarrow{GS_3} = [-\frac{1}{2}r_p, -\frac{\sqrt{3}}{2}r_p, 0]^T$ . The position vector of the spherical joints with respect to the co-ordinate system  $\{X_1, Y_1, Z_1\}$  is given as

$$\begin{bmatrix} \overrightarrow{O_1 S_i} \\ 1 \end{bmatrix} = [T] \begin{bmatrix} \overrightarrow{GS_i} \\ 1 \end{bmatrix}$$

The leg lengths can be found out as shown in reference [3] as

$$l_i = \|\overrightarrow{O_1 R_i} - \overrightarrow{O_1 S_i}\|$$

where  $i = 1, 2, 3$  and  $\|\cdot\|$  represents the norm of the vector.

In the next section, we present a finite element method based modeling of the mirror and the support structure to determine deflections due to wind loading and self weight.

### 3 Finite element modeling of mirror and support structure

The finite element analysis of the mirror and support structure is done in ANSYS<sup>®</sup> Workbench [8]. The element types used are *SOLID186* and *SOLID187* with three degrees of freedom per node. Program controlled automatic

$$\left( -12 \frac{a_2^2 y_c^2}{a_1^2 r_p^4} - 4 \frac{y_c^2}{r_p^4} - 4 \frac{a_2^4 y_c^2}{a_1^4 r_p^4} + 4 \frac{a_2^2}{r_p^2 a_3^2} - 4 \frac{a_2^4 y_c^2}{r_p^4 a_3^2 a_1^2} + 4 \frac{a_2^2}{a_1^2 r_p^2} - 8 \frac{a_3^2 a_2^2 y_c^2}{a_1^4 r_p^4} - 4 \frac{a_2^2 y_c^2}{r_p^4 a_3^2} - 4 \frac{a_3^4 y_c^2}{a_1^4 r_p^4} - 8 \frac{a_3^2 y_c^2}{a_1^2 r_p^4} \right) x_c^2 +$$

$$\left( 4 \frac{y_c^3 a_2^5}{r_p^4 a_1^3 a_3^2} - 4 \frac{y_c a_2^3}{r_p^2 a_1 a_3^2} + 4 \frac{a_3^2 y_c a_2}{a_1^3 r_p^2} + 4 \frac{y_c^3 a_2^3}{r_p^4 a_1^3} + 4 \frac{a_1 y_c a_2}{r_p^2 a_3^2} - 4 \frac{a_1 y_c^3 a_2}{r_p^4 a_3^2} + 8 \frac{y_c a_2}{r_p^2 a_1} - 4 \frac{y_c^3 a_2}{r_p^4 a_1} \right) x_c +$$

$$5 \frac{y_c^2}{r_p^2} + 2 \frac{a_2^2 y_c^2}{a_1^2 r_p^2} + \frac{a_2^4 y_c^2}{r_p^2 a_1^4} - \frac{a_2^2}{a_1^2} - 4 \frac{a_3^4 y_c^4}{a_1^4 r_p^4} + 8 \frac{a_3^2 y_c^2}{a_1^2 r_p^2} - 8 \frac{a_3^2 y_c^4}{a_1^2 r_p^4} - 5 \frac{y_c^4}{r_p^4} + \frac{a_1^2 y_c^2}{r_p^2 a_3^2} - \frac{a_1^2 y_c^4}{r_p^4 a_3^2} - 5 \frac{y_c^4 a_2^4}{a_1^4 r_p^4} - 6 \frac{y_c^4 a_2^2}{a_1^2 r_p^4} + 4 \frac{a_3^2 a_2^2 y_c^2}{r_p^2 a_1^4}$$

$$- 8 \frac{y_c^4 a_3^2 a_2^2}{a_1^4 r_p^4} - 2 \frac{a_2^2 y_c^2}{r_p^2 a_3^2} + \frac{y_c^4 a_2^2}{r_p^4 a_3^2} + 4 \frac{a_3^4 y_c^2}{r_p^2 a_1^4} + \frac{y_c^4 a_2^4}{r_p^4 a_3^2 a_1^2} - \frac{y_c^4 a_2^6}{r_p^4 a_1^4 a_3^2} + \frac{a_2^4 y_c^2}{r_p^2 a_1^2 a_3^2} = 0 \quad (14)$$

$$\left( -4 \frac{y_c^2}{r_p^4} - 8 \frac{a_3^2 a_2^2 y_c^2}{a_1^4 r_p^4} + 4 \frac{a_2^2}{a_1^2 r_p^2} - 4 \frac{a_2^4 y_c^2}{r_p^4 a_3^2 a_1^2} - 4 \frac{a_2^2 y_c^2}{r_p^4 a_3^2} - 4 \frac{a_3^4 y_c^2}{a_1^4 r_p^4} - 8 \frac{a_3^2 y_c^2}{a_1^2 r_p^4} - 4 \frac{a_2^4 y_c^2}{a_1^4 r_p^4} - 12 \frac{a_2^2 y_c^2}{a_1^2 r_p^4} + 4 \frac{a_2^4}{r_p^2 a_1^2 a_3^2} \right) x_c^2 +$$

$$\left( -8 \frac{y_c a_2^3}{a_1^3 r_p^2} + 4 \frac{y_c a_2^3}{r_p^2 a_1 a_3^2} - 4 \frac{a_2^5 y_c}{a_1^3 a_3^2 r_p^2} - 4 \frac{y_c^3 a_2}{r_p^4 a_1} - 4 \frac{a_1 y_c^3 a_2}{r_p^4 a_3^2} + 4 \frac{y_c^3 a_2^5}{r_p^4 a_1^3 a_3^2} - 4 \frac{a_3^2 y_c a_2}{a_1^3 r_p^2} + 4 \frac{y_c^3 a_2^3}{r_p^4 a_1^3} \right) x_c +$$

$$\frac{y_c^2}{r_p^2} + 2 \frac{a_2^2 y_c^2}{a_1^2 r_p^2} + 4 \frac{a_3^4 y_c^2}{r_p^2 a_1^4} - \frac{a_2^2}{a_1^2} + 4 \frac{a_3^2 y_c^2}{a_1^2 r_p^2} - 8 \frac{a_3^2 y_c^4}{a_1^2 r_p^4} - 5 \frac{y_c^4}{r_p^4} - \frac{a_1^2 y_c^4}{r_p^4 a_3^2} - 6 \frac{y_c^4 a_2^2}{a_1^2 r_p^4} + 8 \frac{a_3^2 a_2^2 y_c^2}{r_p^2 a_1^4} - 8 \frac{y_c^4 a_3^2 a_2^2}{a_1^4 r_p^4} - 5 \frac{y_c^4 a_2^4}{a_1^4 r_p^4} +$$

$$5 \frac{a_2^4 y_c^2}{r_p^2 a_1^4} - \frac{y_c^4 a_2^6}{r_p^4 a_1^4 a_3^2} + \frac{y_c^4 a_2^4}{r_p^4 a_3^2 a_1^2} + \frac{a_2^2 y_c^2}{r_p^2 a_3^2} - 4 \frac{a_3^4 y_c^4}{a_1^4 r_p^4} + \frac{y_c^4 a_2^2}{r_p^4 a_3^2} - 2 \frac{a_2^4 y_c^2}{r_p^2 a_1^2 a_3^2} + \frac{a_2^6 y_c^2}{a_1^4 a_3^2 r_p^2} = 0 \quad (15)$$

## 2.2 Determination of leg lengths

From the geometry of the 3-RPS manipulator, the co-ordinates of the revolute joints with respect to  $\{X_1, Y_1, Z_1\}$  are given by  $\overrightarrow{O_1 R_1} = [r_b, 0, 0]^T$ ,  $\overrightarrow{O_1 R_2} = [-\frac{1}{2}r_b, \frac{\sqrt{3}}{2}r_b, 0]^T$  and  $\overrightarrow{O_1 R_3} = [-\frac{1}{2}r_b, -\frac{\sqrt{3}}{2}r_b, 0]^T$  and the co-ordinates of the spherical joints with respect to  $\{x, y, z\}$  are given

meshing is enabled for the analysis. The mesh size is refined in each iteration until convergence is achieved. The deformation of the mirror and support structure is found out for its self-weight and a survival wind speed,  $v$  of 22 m/s.

The structure is kept vertically so that the worst case scenario can be simulated. The factor of safety ( $FoS$ ) used for the analysis is 2. The uniform wind load ( $P$ ) on the

surface of the mirror is calculated by using the equation,

$$P = \frac{1}{2} C_d \rho v^2 F_o S$$

where  $C_d = 1.18$  is the drag coefficient and  $\rho$  is the density of air assumed to be  $1.25 \text{ kg/m}^3$ .

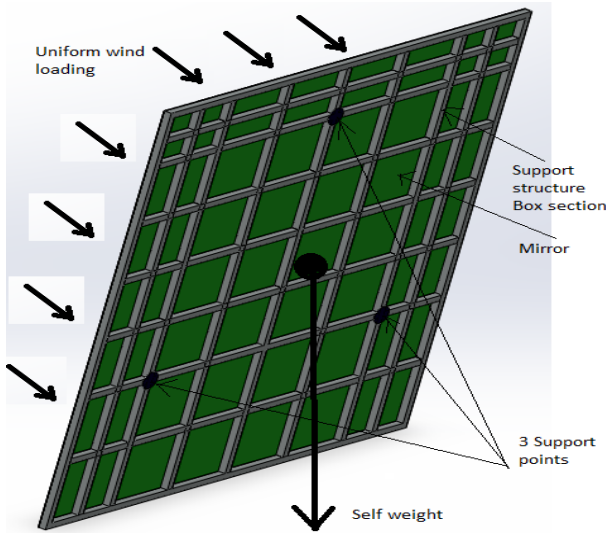


**Figure 2: Uniform wind load acting on the mirror**

The mirror is assumed to be made of float glass and weighing  $10 \text{ kg/m}^2$  and we have created models of various sizes – results for  $2\text{m} \times 2\text{m}$ ,  $3\text{m} \times 3\text{m}$  and  $5\text{m} \times 5\text{m}$  are presented. We have attempted various configurations of support structures and supporting material, made of low carbon steel, of different cross-section and wall thickness. The CAD model of the support structure and the mirror was made using SolidWorks® [9] and the two were mated to obtain a single object and then ported to ANSYS® for finite element analysis to obtain the stresses and deformation due to the wind and self-weight loading. The goal of the continuing study is to obtain the lightest support structure which satisfies the maximum deformation requirements and thus reduce material cost. We present representative results in the next section.

#### 4 Simulation results

In this section, we present numerical simulation results for the motion of the heliostat to track the sun. We also present finite element analysis to determine deflection of various sized mirrors due to wind load and self-weight.

As mentioned earlier the motion of the sun in the sky depends on the date and time of the year and also on the latitude and longitude of the location on Earth. We present simulation results for 6th of May 2013 and for Bangalore, India (Latitude  $12^\circ 58' 13'' \text{ N}$  and Longitude  $77^\circ 33' 37'' \text{ E}$ ). The motion of the 3-RPS based heliostat for different instants of time is simulated in MATLAB® and is shown in Fig.3. For  $r_p$  and  $r_b$  equal to 1m, the leg lengths of the 3-RPS based heliostat are computed and shown in Fig.4. To focus the sun rays on to the receiver kept at  $(0, 0, 65\text{m})$  with

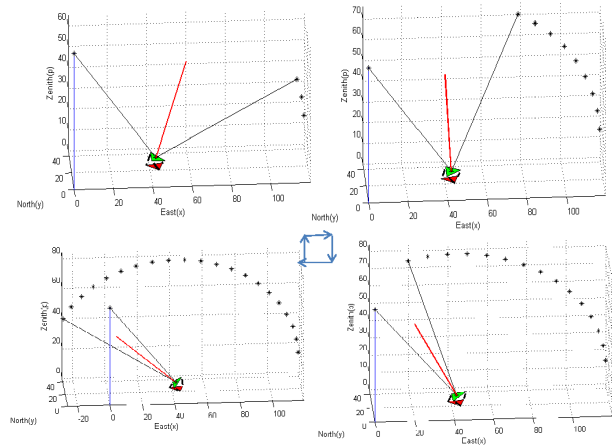


**Figure 3: Motion of 3-RPS heliostat with time**

respect to the fixed co-ordinate system, the actuated joints of the 3-RPS manipulator needs to be moved as shown in Fig. 4.

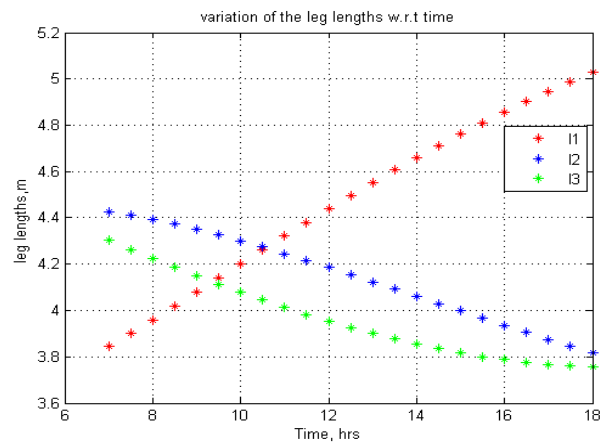


**Figure 4: Variation of leg lengths with time**

Fig. 5, Fig. 6 and Fig. 7 shows the finite element analysis results for three heliostats. Table 1, shows the maximum deformation in each of the three heliostats and the weight of the support structure. The details of the sections used for the finite element analysis are as follows:

- For  $2\text{m} \times 2\text{m}$  the results are for square box section of size 30 mm and wall thickness of 2 mm.
- For  $3\text{m} \times 3\text{m}$  the results are for square box section of size 50 mm and wall thickness of 2 mm.
- For  $5\text{m} \times 5\text{m}$  the results are for square box section of size 70 mm and wall thickness of 3 mm.

The maximum stress values are not shown as they are very small and the maximum deformation is of interest. For comparison, we also made finite element models of each of the three heliostat with single point support thus simulating the currently used Azimuth-Elevation and Target-Aligned

system of actuation. From the figures and tables, it can be seen that the slope error is less than 2 mrad everywhere. It can also be seen the weight of the support structure is much less with the three point support available when the parallel 3-RPS manipulator is used. It maybe noted that for the specification of operation at the wind speed of 10 m/s, the maximum deflection are lower – they are 1.07 mm, 2.96 mm and 4.86 mm for 2m × 2m, 3m × 3m , 5m × 5m mirror sizes, respectively.

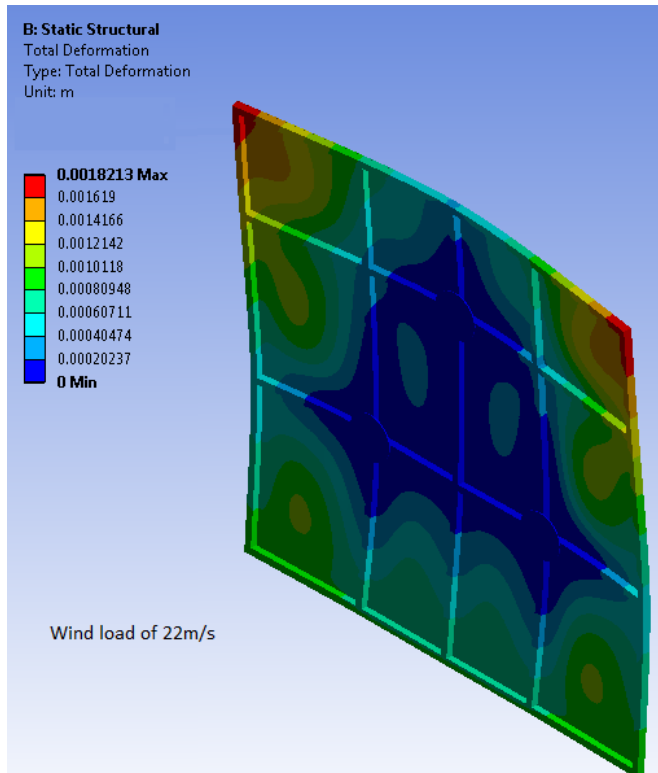


Figure 5: Deformation of a 2m x 2m mirror.

Table 1: Comparison of weight and deflection for 3-RPS and Single Point Support (SPS)

Mirror size (m x m)	Support structure weight ( kg )		Deflection (mm)	
	3-RPS	SPS	3-RPS	SPS
2 x 2	30	35.5	1.82	1.93
3 x 3	93	181.2	2.66	2.87
5 x 5	535	1273	4.92	4.86

## 5 Conclusions and challenges ahead

This paper deals with the use of a parallel three degree-of-freedom parallel manipulator, the well-known 3-RPS, for tracking the motion of the sun for concentrated solar power application. It is shown that the parallel manipulator can be used as a heliostat and it has several features better than the conventional Azimuth-Elevation and Target-Aligned serial configurations. The two main advan-

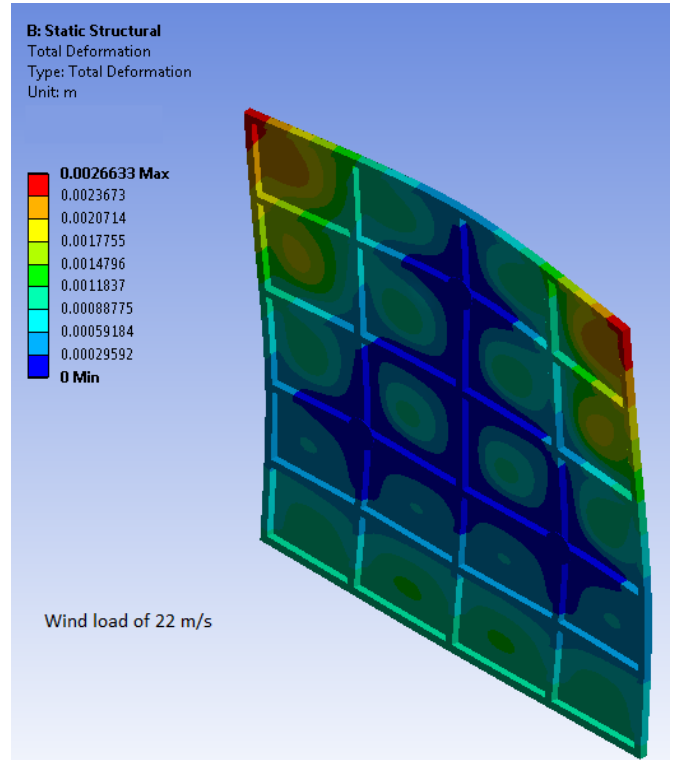


Figure 6: Deformation of a 3m x 3m mirror.

tages follows from the advantages of parallel manipulators over serial manipulators, namely larger load carrying capabilities and more accuracy. It is shown that the weight of the support structure in the parallel 3-RPS manipulator is about a half to one third of the support structure of the commonly used Azimuth-Elevation configuration to meet the same maximum deflection criterion. It is expected that this will lead to development of larger heliostats and thus the cost per square meter of heliostats may be reduced even though the parallel manipulator requires one additional actuator. Another key advantage of the parallel 3-RPS based heliostat is that due to the use of prismatic joints or linear actuators, the requirement of accurate gears and expensive gear reduction systems can be significantly reduced and this may further reduce the cost of the heliostats.

The work reported in this paper is continuing. One of the major challenges is to find a good way to fix the mirror(s) to the support structure and to obtain an optimum value for the radius of the circumscribing circle  $r_p$ . A change in  $r_p$  value not only changes the stroke of the linear actuators but also the maximum deformation at the edges of the mirror. If the value of  $r_p$  is large, the prismatic joints have to be moved more to get the required orientation of the moving platform and if it is less, then the deformation at the edges will be large. Another issue is to make use of the third degree of freedom available in the 3-RPS manipulator, namely the translational motion along the vertical direction, in interesting ways. In this work, we have fixed the vertical coordinate arbitrarily. However, optimization of a useful objective function can also be explored.

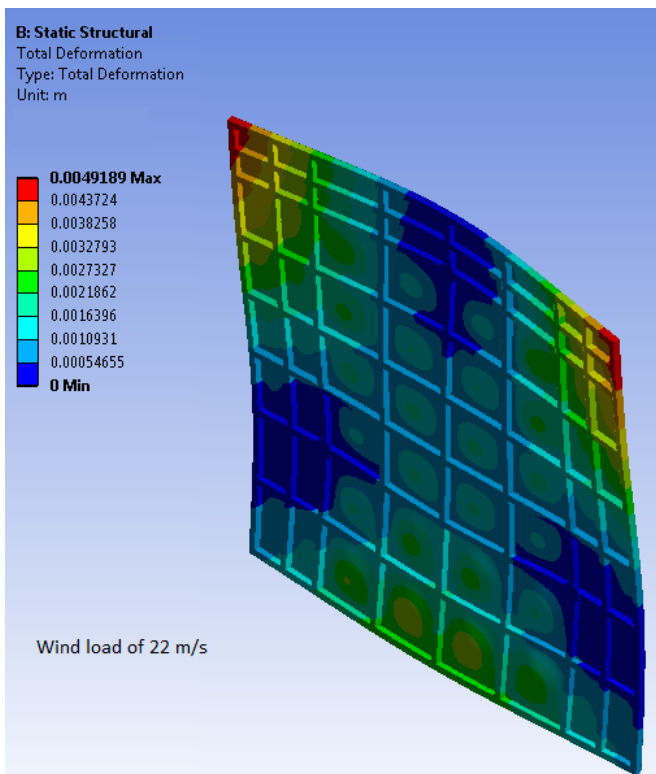


Figure 7: Deformation of a 5m x 5m mirror.

### Acknowledgement

This work has been partly funded by a grant from the Solar Energy Research Institute for India and the United States (<http://www.serius.org>). The authors would also like to thank Mohit Acharya who helped in obtaining results relating to maximum deflection of the mirror assembly for the Azimuth-Elevation configuration.

### References

1. L.L. Vant-Hull, 8 - Central tower concentrating solar power (CSP) systems, In Woodhead Publishing Series in Energy, edited by Keith Lovegrove and Wes Stein, Woodhead Publishing, 2012, Pages 240-283, Concentrating Solar Power Technology, ISBN 9781845697693
2. Xiudong Wei, Zhenwu Lu, Weixing Yu, Hongxin Zhang, Zhifeng Wang, Tracking and ray tracing equations for the target-aligned heliostat for solar tower power plants, Renewable Energy, Volume 36, Issue 10, October 2011, Pages 2687-2693.
3. Ghosal A., Robotics Fundamental Concepts and Analysis, Oxford University Press, 2006.
4. Lee, K.-M. and Shah, D., Kinematic analysis of three degrees of freedom in-parallel actuated manipulator, IEEE J. of Robotics and Automation, Vol. 4, Issue 2, pp. 354-360, 1988.
5. Srivatsan, R. Arun, Bandyopadhyay, S. and Ghosal, A., Analysis of the degrees-of-freedom of spatial parallel manipulators in regular and singular configurations, Mechanism and Machine Theory, Vol. 69, pp. 127-141, 2013.

6. <http://pveducation.org/pvcdrom/properties-of-sunlight/azimuth-angle>
7. MATLAB. version 7.12.0 (R2011a). The MathWorks Inc., Natick, Massachusetts, 2012.
8. ANSYS Workbench, Ansys Inc., Pennsylvania, USA
9. SolidWorks, Dassault Systems, Vlizy, France.